Journal Name

ARTICLE

Impact of α-hydrazino acids embedded in short fluorescent peptides on peptide interaction with DNA and RNA

Received 00th January 20xx,
Accepted 00th January 20xx

DOI: 10.1039/x0xx00000x

www.rsc.org/

Josipa Suć,[a] Lidija-Marija Tumir,[a] Ljubica Glavaš-Obrovac,[b] Marijana Jukić,[b] Ivo Piantanida [a]* and Ivanka Jerić [a]*

Series of novel hydrazino-based peptidomimetics and analogues comprising N-terminal lysine and C-terminal phenanthridinyl-L-alanine were prepared. Presented results demonstrate up till now unknown possibility to finely modulate peptide interaction with DNA/RNA by α-hydrazino group insertion and how different positioning of two α-hydrazino groups in peptide controls binding to various double stranded and single stranded DNA and RNA. All peptidomimetics bind with 1-10 micromolar affinity to ds-DNA/RNA, whereby binding mode is combination of electrostatic interactions and hydrophobic interactions within DNA/RNA grooves. Insertion of α-hydrazino group into peptide systematically decreased its fluorimetric response to DNA/RNA binding in line: mono-hydrazino<alternating-hydrazino< sequential-hydrazino group. Binding studies to ss-polynucleotides suggest intercalation of phenanthridine between polynucleotide bases, whereby affinity and fluorimetric response decrease with the number of α-hydrazino groups in peptide sequence. Particularly interesting was interaction of two sequential α-hydrazino acids-peptidomimetic with poly rG, characterised by specific strong increase of CD bands, while all other peptide/ssRNA combinations gave only CD-bands decrease. All mentioned interactions could also be reversibly controlled by pH, due to the protonation of the fluorophore.

Introduction

The life is characterised by extremely complex system of interactions between proteins, DNA, RNA, and many small molecules. These interactions frequently take place at structurally well-defined regions formed by protein backbone folding. There is a great interest in mimicking folded protein epitopes by small molecules,[1,2] biologically active peptides,[3] cyclic peptides,[4,5] or peptidomimetics.[6,7] While short peptides comprising α-amino acids generally fail to form thermodynamically stable secondary structures, backbone extended peptidomimetics comprising β- or γ-amino acids, aminoxy or hydrazino acids readily adopt ''protein-like'' secondary structures, such as helices, sheets and turns.[8,9] β-Peptides and oligomers containing mixtures of α- and β-amino acids have been extensively studied as inhibitors of protein-protein interactions.[10,11,12] Replacement of Cβ atom in β-amino acids with nitrogen leads to hydrazino peptides, a class of peptidomimetics characterized by an array of intramolecular hydrogen bonds that are responsible for various secondary structures.[8,13,14] Although hydrazino-based peptidomimetics showed promising biological activities,[15,16] their wider exploitation is hampered by somewhat challenging synthesis. However, it was shown recently by our group and others,[17] that unprotected hydrazino acids can be successfully applied in synthesis of hybrid hydrazino peptidomimetics, thus enabling progress in utilization of this class of compounds.

A number of short natural and synthetic peptides target DNA/RNA, among which condensed aromatic-peptide conjugates attracted quite a lot of attention in the last decade.[18] In general, condensed-aromatic part contributed to DNA/RNA binding by intercalation and was responsible for spectrophotometric monitoring of interaction. However, selectivity was usually controlled by hydrogen bonding pattern along peptide backbone within one of DNA/RNA grooves.[18,19] To the best of our knowledge, hydrazino acids were never incorporated within DNA/RNA targeting compounds, although hydrazino moiety is well-directed double hydrogen donor. Moreover, incorporation of one or more hydrazino-based residues within short peptides can affect peptide secondary structure. Acherar et al. found that, owing to the H-bond donor and acceptor character of amidic NH, hybrid oligomers composed of α-amino and α-hydrazino acids can adopt multiple conformations.[14] We presumed that such conformational adaptability could be important for steric control and pre-organisation before binding to DNA/RNA. To address aforesaid features, we prepared small series of hydrazino-based peptidomimetics, **1-4** (Figure 1), whereby number and position of α-hydrazino residues are systematically varied, while keeping constant the position of

a Division of Organic Chemistry and Biochemistry, Ruđer Bošković Institute, Bijenička cesta 54, 10000 Zagreb, Croatia
b Department of Medicinal Chemistry and Biochemistry, School of Medicine Osijek,31000 Osijek, Croatia

†Electronic Supplementary Information (ESI) available: [NMR and HRMS spectra of **1-4**, spectroscopic properties (UV/Vis and fluorescence spectra, interactions of **1-4** with DNA/RNA (thermal denaturation experiments, fluorimetric titration curves, CD spectra) , cytotoxicity data]. See DOI: 10.1039/x0xx00000x

positively charged lysine (expected to contribute to the DNA/RNA binding by electrostatic interactions), and fluorescent phenanthridinyl-L-alanine (AlaP) (contributing to DNA/RNA binding and reporting the recognition by fluorescence).

Results and discussion

Synthesis

Peptides comprising single hydrazino-L-leucine (hLeu) residue (**2**), two sequential hLeu residues (**3**) and alternating residues (**4**) were prepared by solution-phase methodology. Pentapeptide **1** with incorporated AlaP was prepared to distinguish contributions of a large condensed aromatic unit and hydrazino acids on binding. Generally, peptidomimetics were prepared by fragment assembly strategy (Figure 1). Tripeptides **5**, **7** and **9** were synthesized according previously developed methodologies[17~~17~~a] and coupled to C-terminal dipeptide comprising AlaP. In the final step, terminal protecting groups were cleaved and crude products purified by HPLC.

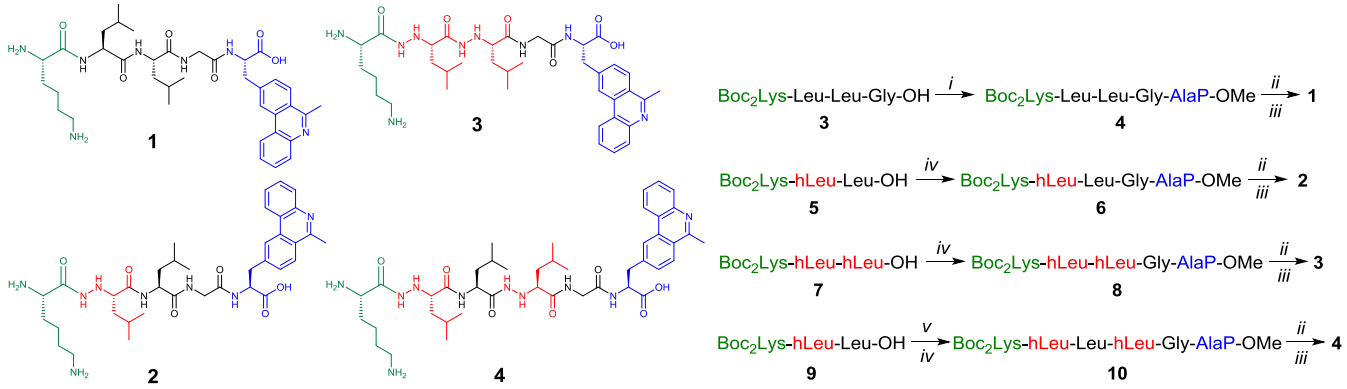

Figure 1. Structures of hydrazino peptides (left) and preparation outline (right): i) HATU, NMM, H-AlaP-OMe in DMF, 24 h, RT; (ii) 1M NaOH, MeOH, 65 °C, 2 h; (iii) TFA:H_2O = 9:1, RT, 1 h; (iv) HATU, NMM, H-Gly-AlaP-OMe in DMF, 24 h, RT; (v) DCC, HOSu, H-hLeu-OH, in DMF, 24 h, RT.

Physical-chemical and spectroscopic properties of aqueous solutions of 1-4

Studied compounds **1-4** are soluble in redistilled water (up to $c = 1 \times 10^{-2}$ M), and aqueous solutions were stable over 6 months. Absorbances of **1-4** aqueous solutions were proportional to their concentrations up to $c = 2\text{-}4 \times 10^{-5}$ M and didn't change notably up to 90 °C, indicating that there is no significant inter- or intramolecular aromatic stacking, which should give rise to hypochromicity effects. Fluorescence emissions of **1-4** were linearly dependent on their concentrations up to $c = 6 \times 10^{-6}$ M. Spectroscopic characterisation is given in ESI† (Figures S1-S18†). It is noteworthy that at pH 5 phenanthridine moiety is mostly protonated, which influences to some extent spectroscopic properties of **1-4**, in line with previous data.[20,21] Studies of interactions with DNA and RNA were done at both, pH 7 and pH 5, acidic conditions yielding stronger effects and thus discussed in detail within the manuscript.

DNA/RNA binding studies

Here used AlaP was previously combined with amino acids (Gly and thyminyl-L-alanine, AlaT) and simple dipeptide (Gly-Gly) to give moderate binding effects on ds-DNA/RNA thermal stability and CD properties.[22] The incorporation of hydrazino acid(s) at various positions in a peptide flanked by lysine on one side (for electrostatic attraction with DNA/RNA backbone) and by AlaP on opposite side, was expected to have significant impact on positioning and binding of phenanthridine chromophore to ds-DNA/RNA. Indeed, at both, pH 5 and pH 7, **1-4** didn't thermally stabilise any ds-DNA/RNA (Table S1†, Figures S19-S21†). Therefore, intercalative binding mode (common for AlaP[2~~22~~2]) can be excluded. To get better structural insight into **1-4** /ds-DNA/RNA complexes, we used CD spectroscopy as a highly sensitive method for conformational changes in the secondary structure of polynucleotides.[23] Moreover, small molecule chromophores (e.g. AlaP in **1-4**), could upon binding to DNA or RNA acquire induced (I)CD spectrum, which could be helpful in determination of binding mode (intercalation, groove binding, agglomeration, etc.).[24,25] However, negligible changes in CD spectra of ds-polynucleotides (Figures S23-S34†) and absence of any induced (I)CD bands > 300 nm, pointed out that phenanthridine-chromophore does not bind in one well-defined orientation in respect to DNA/RNA chiral axis. However, fluorimetric response (Figure 2, ΔI in Table 1, Figures S51-S54 ESI†) and also binding affinity (Ks, Table 1) of **1-4** to ds-DNA/RNA were both strongly sensitive on the number of hydrazino groups in peptide. Even more, peptidomimetic **3** with two adjacent hydrazino acids showed lower binding affinity as well as smaller fluorescence response than peptidomimetic **4** with alternating distribution of hydrazino acids. Also, binding constants were order of magnitude higher at pH 5 (Table 1) than at pH 7 (Table S2 ESI†) due to the protonation of phenanthridine moiety at acidic conditions,

additional positive charge contributing to the electrostatic component of binding[2020].

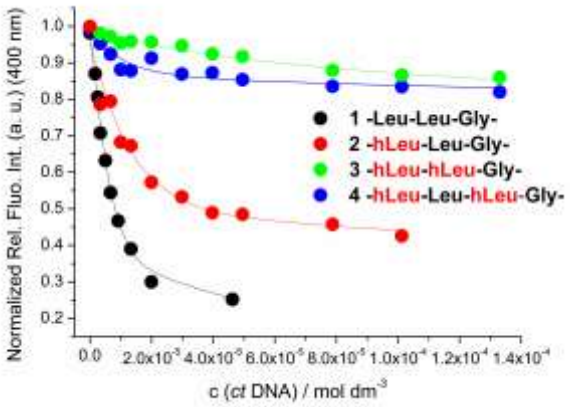

Figure 2. Experimental (●) and calculated (–) (by Scatchard eq., Table 1) fluorescence intensities of compounds **1-4** upon addition of ct-DNA; note various positions of hydrazino-L-leucine (**hLeu**); Na-cacodylate buffer, pH 5.0, *I* = 0.05 M, λ_{exc} = 310 nm.

Table 1. Stability constants (log*Ks*)[a] and spectroscopic properties of complexes ΔI [b] of **1-4** with ds-polynucleotides calculated according to fluorimetric titrations (Na-cacodylate buffer, c = 0.05 M, pH = 5.0; λ_{exc}= 310 nm, λ_{em}= 350 – 500 nm, c(**1-4**) = 1-2 × 10^{-6} M).

	ct-DNA	poly (dA-dT)$_2$	poly (dG-dC)$_2$	poly A-poly U
	log *Ks*[a]/ΔI[b]	log *Ks*[a] / ΔI[b]	log *Ks*[a] / ΔI[b]	log *Ks*[a] / ΔI[b]
1	6.5 / -78%	6.4 / -80%	6.4 / -81%	5.9 / -75%
2	6.2 / -55%	6.1 /-61%	6.1 / -62%	5.9 / -38%
3	5.1 /-20%	5.1 /-21%	4.9 /-35%	[c]
4	>6[d] /-12%	6.1 /-24%	5.9 /-34%	5-6[d] /-15%

[a] Processing of titration data by Scatchard equation[26] gave values of ratio n [bound peptide] / [polynucleotide] = 0.15 ± 0.05 for most complexes; for easier comparison values of log *Ks* are recalculated for fixed n=0.15; correlation coefficients were >0.98-0.99 for all calculated *Ks;* [b] Changes of fluorescence of compound **1-4** induced by complex formation ($\Delta I = (I_{lim} - I_0) \times 100 / I_0$; where I_0 is emission intensity of free compound and I_{lim} is emission intensity of a complex calculated by Scatchard eq.); [c] Too small and linear fluorescence change hampered calculation of *Ks*; [e] Small total emission change allowed only estimation of *Ks*.

All afore mentioned suggests that **1-4** bind externally to ds-DNA/RNA, whereby binding forces are not exclusively electrostatic: two positive charges (Lys and AlaP) should give log*Ks* < 4[27] and only four and more positive charges could yield log*Ks* ≥ 6[28]. That supports significant contribution of hydrophobic interactions of both, neutral peptide linker and also large aromatic fluorophore, whereby better part of the molecule is buried within hydrophobic DNA/RNA grooves. Hydrophobic binding contribution in combination with various steric properties of hydrazino-residues is significant since it controls position of fluorophore yielding differences in fluorimetric response (**1**>**2**>**4**>**3**) and binding affinity.

Comparison of all obtained results revealed that presence of Nα-unsubstituted hLeu impairs the interactions of **2-4** (compared to **1**) by withdrawing the fluorophore from the DNA/RNA binding site. When more exposed to water and less in binding contact with DNA/RNA, AlaP fluorescence is less quenched. The explanation for such outcome can be found in conformational preferences of peptides with incorporated α-hydrazino acids, which are able to self-organize through intramolecular hydrogen bonding network in solution. For instance peptides with Nα-substituted hydrazino acids show "hydrazino-turns", eight-membered hydrogen-bonded pseudocycles.[29,30] Furthermore, CD spectra of terminally protected hydrazino hexamer composed of hLeu and hAla resembles structural characteristics of β-peptides, namely right-handed helical secondary structure.[31] Acherar et al. undertook in-depth secondary structure analysis of oligomers composed of alternating α-amino acids and Nα-unsubstituted hydrazino acids and reported that the major conformer present is in equilibrium between pseudospiranic and hydrazino-turn conformation.[14]

Detailed analysis of **1-4**/DNA complexes by structurally more informative method like NMR spectroscopy was hampered by severe peak overlapping of amide and hydrazino protons (similar as noted by Lelais and Seebach[30] as well as insufficient solubility of compound complexes with DNA/RNA.

Molecular modelling in water of such peptides and their DNA/RNA complexes is very demanding task due to the high flexibility of peptides and mutual changing of structure upon binding; therefore full profile modelling is out of the scope of this work. However, in attempt to at least visualise the structural features which could explain our experimental results, we submitted **1-4** to MM2 calculations by a modified version of Allinger's MM2 force field, integrated into the ChemBio3D 11.0 programme, whereby obtained structures (Figure S65[†]) demonstrate the possible intramolecular H-bond network for each peptide, and resulting secondary structure. It is noteworthy that structures of **1**, **2** overlap excellently (Figures S66[†]), as well as the structures of bis-hidrazino **3** and **4** (Figures S67[†]), however the differences between these two groups are substantial. Since compounds **1-4** do not alter ds-DNA secondary structure (no change in DNA CD spectra, no thermal stabilisation), we used as ds-DNA model the alternating dAdT-dAdT sequence constructed earlier,[32] Manual docking of **1** and **3** was performed by VMD programme[33], whereby conformational space of small molecule within DNA-binding site was checked that VdW radii of DNA and ligand do not overlap.

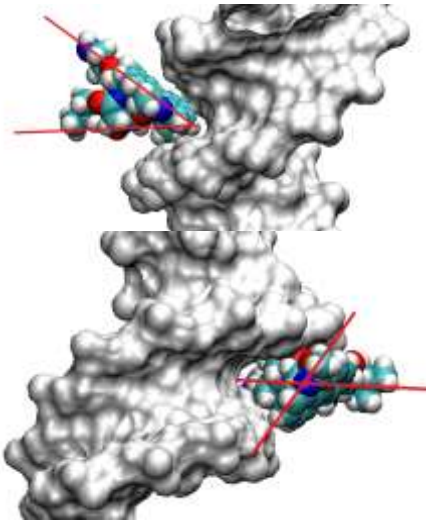

Scheme 1. Schematic presentation of **1** (up) and **3** (down) manually docked into poly dAdT – poly dAdT minor groove. Red lines mark axes positioned along voluminous substituents: AlaP and Leu/Lys chains.

For **1**/DNA complex (Scheme 1, up) it is noteworthy that red lines positioned along longer axis of AlaP and Leu/Lys chains converge into AT-DNA minor groove, giving excellent fit. Hydrophobic area (AlaP+Leu) is pointing inside groove, while hydrophilic part (Lys) is pointing out. At variance to **1**, in **3**/DNA (Scheme 1, down) red lines positioned along longer axis of AlaP and two hLeu side-chains are almost perpendicular, which hampers deep insertion of the molecule into AT-DNA minor groove. Consequently, fluorophore (AlaP) of **1** (and also analogue **2**) could be significantly deeper inserted into DNA minor groove, yielding therefore much stronger fluorimetric change in comparison to **3** and **4**.

Study of interactions of 1-4 with single stranded (ss) polynucleotides

Single stranded (ss) polynucleotides are considerably more flexible than double stranded polynucleotides[34~~34~~]. However, it should be noted that both poly rA and poly rC can form double stranded partially protonated helical structures at pH 5 (namely poly rAH^+ - poly rAH^+ and poly rCH^+ - poly rC).[34] Also, poly rG can form complex intrastrand structures and actually only poly rU can be considered as mostly single stranded at all conditions.

Again, fluorimetric response (Figure 3, ΔI in Table 2 and Figure S56-S63 ESI†) and also binding affinity (*Ks*, Table 2) of **1-4** to ss-RNA were strongly sensitive on the number and distribution of hydrazino residues in peptide with similar tendency observed for ds-DNA/RNA (Fig. 2).

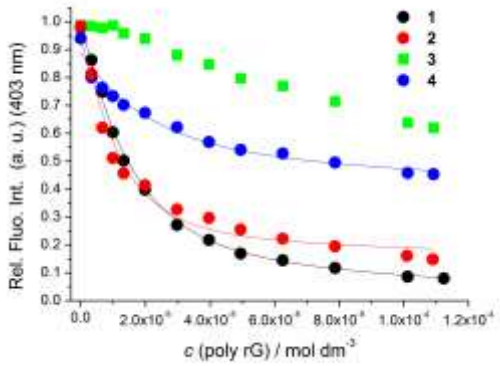

Figure 3. Experimental (•) and calculated (–)(by Scatchard eq., Table 2) fluorescence intensities of compounds **1-4** upon addition of poly G; values were normalized for easier comparison. Na-cacodylate buffer, pH 5.0, *I*= 0.05 M, λ_{exc} = 310 nm.

Affinities of **1-4** toward single stranded polynucleotides were similar at pH 5 (Table 2~~Table 2~~) and pH 7 (Table S3 ESI†), thus not depending on AlaP protonation state. Since aromatic stacking interactions are usually not dependent on aryl-charge, this suggested intercalation of AlaP between polynucleotide bases. That was additionally supported by significantly stronger fluorescence quenching of all peptides with poly rA, poly rG compared to poly rU, poly rC polynucleotides (Table 2~~Table 2~~), attributed to more efficient aromatic stacking interactions between AlaP and larger purine nucleobase in respect to smaller pyrimidine. Again, number and vicinity of hydrazino groups affects affinities and fluorimetric response in line **1**>**2**>**4**>**3** (Figure 3, Figure S56-S63 ESI†).

Table 2. Stability constants ($\log K_s$)[a] and spectroscopic properties of complexes ΔI[b] of **1-4** with ss-polynucleotides calculated according to fluorimetric titrations (Na-cacodylate buffer, c = 0.05 M, pH = 5.0; λ_{exc}= 310 nm, λ_{em}= 350 – 500 nm, c(**1-4**) = 1-2 × 10^{-6} M).

	poly A	poly G	poly U	poly C
	log *Ks*[a]/ΔI[b]	log *Ks*[a] / ΔI[b]	log *Ks*[a] / ΔI[b]	log *Ks*[a] / ΔI[b]
1	5.3 / -64%	5.9 / -98%	>6[c]/ -12%	>6[c] / -19%
2	5.9 / -42%	6.2 / -82%	>5[c] / -10%	>6[c] / -9%
3	5.3 / -10%	[d]	[d]	[d]
4	5-6[c] / -12%	5.7 /-53%	5-6[c] / -5%	5-6[c] / -8%

[a] Processing of titration data by Scatchard equation[26~~26~~] gave values of ratio n [bound peptide] / [polynucleotide] = 0.15 ± 0.05 for most complexes; for easier comparison values of log *Ks* are recalculated for fixed n=0.15; correlation coefficients were >0.98-0.99 for all calculated *Ks;* [b] Changes of fluorescence of compound **1-4** induced by complex formation ($\Delta I = (I_{lim} - I_0) \times 100 / I_0$; where I_0 is emission intensity of free compound and I_{lim} is emission intensity of a complex calculated by Scatchard eq.); [c] Small total emission change allowed only estimation of *Ks*; [d] Too small and linear fluorescence change / no fluorescence change hampered calculation of *Ks*.

CD spectropolarimetry was applied for detailed structural analysis of complexes[24~~24~~,25~~25~~]. At acidic conditions (pH 5, protonated AlaP) addition of **1-4** resulted in much stronger CD response of ss-RNA (Figures 4, 5) in respect to pH 7 (Figures S35-S50 ESI†), thus only results obtained at pH 5 were further discussed.

Minor decrease within 250-300 nm region could be attributed to intercalation of phenanthridine, which should yield weak negative ICD band[25~~25~~] around its absorption maximum (250 nm, Figure 4) as well as deformation of polynucleotide helical structure causing general RNA-CD bands decrease.[23~~23~~,25~~25~~] Both expected changes could explain the observed decrease of CD spectra upon formation of poly rA/**1-4** complexes (Figures S35-38†) and poly rG/**1,2,4** complexes (Figure 4). Also, less pronounced decrease in poly rU and poly rC complexes could be attributed to smaller nucleobase size and consequently less-efficient aromatic stacking with phenanthridine.

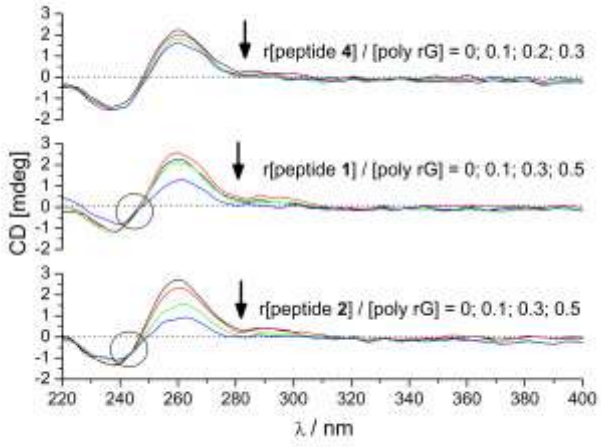

Figure 4. CD titration of poly G (c = 2 × 10^{-5} M) with **1,2,4** at different molar ratios **r** = [compound] / [poly G]. Note isodichroic point in circle. Done at pH = 5.0, sodium cacodylate buffer, *I* = 0.05 M.

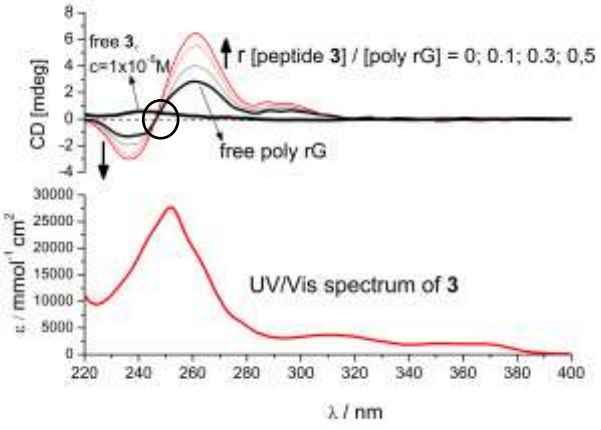

Figure 5. CD titration of poly G (c = 2 × 10^{-5} M) with **3** at different molar ratios **r** = [compound] / [poly G]. Note isodichroic point in circle. Done at pH = 5.0, sodium cacodylate buffer, *I* = 0.05 M.

However, as a unique exception, peptidomimetic **3** yielded strong increase of all CD bands (Figure 5), whereby isoelliptic point in poly rG/**3** titration strongly supported formation of only one type of a complex.

Throughout here presented study, **3** showed the lowest fluorescence increase for all ds-DNA/RNA and in particularly for most ss-RNA, which could be attributed to the rigidity of peptide structure due to two sequential hLeu residues. Since hydrazino peptides can be considered an extension of β-peptide concept, possible secondary structures of hydrazino peptides can be compared with those of β-peptides.[35] It is well documented that systematic combination of α- and β- amino acids generates new secondary structures.[36,37,38] Thus, mixed α/β peptides were found to adopt various helical secondary structures, depending on chirality, structure and distribution of two structural units. Generally, introduction of α-amino acid increases flexibility as compared with homogeneous β-peptides,[35] therefore it can be presumed that peptide **3** with two sequential hLeu residues is more rigid than **2** and **4** with alternating distribution of Leu and hLeu. Thus, observed strong CD spectrum increase (Figure 5) could be attributed to the switch of the binding mode of poly rG/**3** complex, whereby phenanthridine is not intercalated (as in other ss-RNA) due to steric constrains of two sequential hLeu residues but likely positioned along poly rG chain. Such arrangement could increase RNA chirality by stabilizing helical structure of otherwise not-well organized ss-RNA (thus increasing RNA CD bands) and moreover is likely to be combined with strong positive ICD band of chromophore (Phen) bound at approximately 45^0 angle to RNA chiral axis.[25] The most intriguingly, at pH 7 such increase of poly rG CD spectrum by **3** was much weaker, and didn't change negative band at 240 nm (ESI^+) pointing out that protonation of phenanthridine plays a crucial role, most likely due to electrostatic interactions with negatively charged phosphate backbone (another proof of non-intercalative binding).

Biology

While mixed α/β-peptides are widely exploited for studying inhibition of protein-protein interactions (PPI),[39,42] hydrazino-based peptidomimetics were used to a much lesser extent, mainly as human leukocyte elastase and proteasome inhibitors,[15] or antimicrobial agents.[16] Having in mind that many PPIs are mediated by small peptides, the use of designed peptides and peptidomimetics as modulators of PPI is recognized as promising strategy in drug discovery, but also as probes to elucidate the role of PPI in cell biology.[43]

Phenanthridinium derivatives are often strongly cytotoxic, which renders their applications as dyes in biochemical studies on DNA and RNA.[44] Short peptides also could show considerable cell toxicity. However, both, phenanthridine analogues[45] and peptides are also studied as powerful anticancer drugs. For that reason we screened compounds **1, 2** and **4** for cytotoxic activity against two adenocarcinoma cell lines: cervix (HeLa) and colon (CaCo-2), chronic myeloid leukaemia in blast crisis (K562), and normal epithelial cell line (MDCK1) as well. Results pointed out negligible activity of all studied peptidomimetics (ESI^+, $S64^+$) that reached growth inhibition by 50 % (GI_{50}) just on K562 cells at concentration near or higher than 10^{-4} M. Such low cytotoxicity makes these fluorescent peptides safe dyes for laboratory applications.

Conclusions

Hydrazino peptidomimetics **1**-**4** were prepared to study systematically the impact of hydrazino-L-leucine (hLeu) residue in short peptide sequence linking two common DNA/RNA-interacting moieties: positively charged lysine at the peptide N-terminal part and phenanthridinyl-L-alanine (AlaP) at the peptide C-terminal part, acting as pH-dependent fluorophore.

Comparison of results obtained for **1**-**4** with those reported previously for dipeptides Gly-AlaP and thyminyl-L-alanyl-phenanthridinyl-L-alanine (AlaT-AlaP)[22] revealed that N-terminal peptide part has a great influence on binding mode. Already Lys-Leu-Leu-Gly sequence in **1** caused switch of binding ds-DNA/RNA mode from intercalation, reported for Gly-AlaP and AlaT-AlaP[22], to external binding combined with polynucleotide groove interaction. Moreover, replacement of leucine with hydrazino analogues, their number and distribution along peptide backbone determined binding to ds-DNA/RNA, which was proportionally reported by quenching of AlaP fluorescence in line: **2** (single hLeu) > **4** (two alternating hLeu) > **3** (two sequential hLeu). In addition, all peptides retained moderate (1-10μM) affinity toward ds-DNA/RNA, externally controllable by pH (due to AlaP protonation) by change in order of magnitude. Intriguingly, peptides **1**-**4** showed high affinity toward ss-RNA (comparable to ds-DNA/RNA). Again, fluorimetric response of AlaP was proportional to the number of hLeu in peptide sequence,.i.e. emission quenching tendency decrease in line **1**>**2**>**4**>**3**.

However, the most interesting was specific binding of the peptide **3** with two sequential hLeu to poly rG, which caused unique super-organisation of poly rG characterised by specific response in CD spectrum. In addition, CD response at 240 nm (negative band attributed to poly rG backbone) was observed only at pH 5 but not pH 7, and thus could be switched on and off by non-destructive external stimuli (pH). Such specific spectrophotometric probe for micromolar concentrations of poly rG is to the best of our knowledge not known.

Presented results demonstrate up till now untired possibility to finely modulate peptide interaction with DNA/RNA by α-hydrazino-group insertion and moreover combination of several α-hydrazino-groups within peptide. Given results (along with non-toxicity of these peptidomimetics) encourage further studies in line with combination of multiple α-hydrazino-groups within peptide to completely abolish ds-DNA/RNA binding and still preserve high ss-DNA/RNA affinity with particular emphasis on specific poly G recognition achieved by **3**. This future research would directly address very limited number of small molecules highly selective or specific toward ss-DNA/RNA sequences, whereby they found intriguing biomedical uses, for instance in antiviral and antitumor applications.[46,47] Although there are examples of peptides binding to ss-DNA48, Intriguingly, ss-RNA were strongly underexploited targets, most likely due to larger variety of biologically available forms.[49,50]

Experimental section

Materials and methods

Reactions were monitored by TLC on Silica Gel 60 F254 plates (Merck; Darmstadt, Germany) using detection with ninhydrin. Column chromatography was performed on Silica Gel (Merck, 0.040–0.063). RP HPLC analysis was performed on HPLC system coupled with UV detector; C-18 semipreparative (250 9 8 mm, ID 5 μm) column at flow rate of 1 mL/min, or analytical (150 9 4.5 mm, ID 5 μm) column at flow rate of 0.5 mL/min. UV detection was performed at 254 nm or 270 nm. NMR spectra were recorded on 600 and 300 MHz spectrometers, operating at 150. 92 or 75.47 MHz for 13C and 600.13 or 300.13 MHz for 1H nuclei. TMS was used as an internal standard. Mass spectrometry measurements were performed on HPLC system coupled with triple quadrupole mass spectrometer, operating in positive electrospray ionization (ESI) mode. Spectra were recorded from a 10 μg/mL compound solution in 50 % MeOH/0.1 % FA by injection of 3 μL into the ion source of the instrument by autosampler, at the flow rate of 0.2 mL/min (mobile phase 50 % MeOH/0.1 % FA). HRMS analysis was performed on MALDI-TOF mass spectrometer operating in reflectron mode. Mass spectra were acquired by accumulating three spectra after 400 laser shots per spectrum. Calibrant and analyte spectra were obtained in positive ion mode. Calibration type was internal with calibrants produced by matrix ionization (monomeric, dimeric and trimeric CHCA), with azithromycin and angiotensin II dissolved in α-cyano-4-hydroxycinnamic acid matrix in the mass range m/z 190.0499 to 749.5157 or 1046.5417. Accurately measured spectra were internally calibrated and elemental analysis was performed on Data Explorer v. 4.9 Software with mass accuracy better than 5 ppm. Samples were prepared by mixing 1 μL of analyte methanol solution with 5 μL of saturated (10 mg/mL) solution of α-cyano-4-hydroxycinnamic acid (α-CHCA) and internal calibrants (0.1 mg/mL) dissolved in 50 % acetonitrile/0.1 % TFA. MM2 calculations were performed by a modified version of Allinger's MM2 force field, integrated into the ChemBioOffice 2008 programme. Compounds **3**, **5**, **7** and **9** were prepared according previously developed procedure.[17a]

All measurements were performed in aqueous buffer solution (pH = 5, *I* = 0.05 M, sodium cacodylate/HCl buffer or pH = 7, *I* = 0.05 M, sodium cacodylate/HCl buffer). The UV-Vis spectra were recorded on a Varian Cary 100 Bio spectrometer in quartz cuvettes (1 cm). Fluorescence spectra were recorded on Varian Cary Eclipse fluorimeter in quartz cuvettes (1 cm). Under the experimental conditions used (~ 10-6 M) the absorbance and fluorescence intensities of **1**-**4** were proportional to their concentrations.

Polynucleotides were purchased as noted: poly dGdC – poly dGdC, poly dAdT – poly dAdT, poly A – poly U, poly A, poly G, poly U, poly C (Sigma), calf thymus (ct)-DNA (Aldrich) and dissolved in sodium cacodylate buffer, I = 0.05 M, pH=7. The calf thymus ctDNA was additionally sonicated and filtered through a 0.45 mm filter.[51] Polynucleotide concentration was determined spectroscopically[52] as the concentration of phosphates. The concentration of the stock solution (10 mM) of single stranded poly A at pH 7 was determined by UV absorbance measurement at 258 nm using a molar extinction coefficient (ε) value of 9800 M^{-1} cm^{-1} and it was expressed as the concentration of phosphates. It is important to note that at experimental conditions (pH = 5) poly A and poly C were protonated and formed double helix. The double-stranded conformation of poly A and poly C was obtained by lowering the pH value from the initial value of 7.0 to 5.0 and their concentrations directly derived from the concentration of single stranded polynucleotides (ss-poly A). The formation of ds-poly A and ds-poly C were confirmed by CD and thermal melting experiments.[53,54]

In fluorimetric experiments, excitation wavelengths at λmax ≥ 305 nm were used in order to avoid absorption of excitation light by added polynucleotides. Fluorimetric titrations were performed by adding portions of polynucleotide solution into the solution of the studied compound (c= 2×10^{-6} M). After mixing polynucleotides with studied compounds it was observed in all cases that equilibrium was reached in less than 120 seconds. In following 2-3 hours fluorescence spectra of complexes remained constant. Fluorescence spectra were collected at r < 0.3 (r = (compound) / (polynucleotide)) to assure one dominant binding mode. Data that were processed by means of Scatchard equation[2626] gave values of ratio n [bound compound] / [polynucleotide] in the range 0.07-0.2, but for easier comparison all Ks values were re-calculated for

fixed n=0.15. Calculated values for *Ks* have satisfactory correlation coefficients (>0.99).

CD spectra were recorded on JASCO J815 spectrophotometer at room temperature using appropriate 1 cm path quartz cuvettes with scanning speed of 200 nm/min. Buffer background was subtracted from each spectra, while each spectra was result of three accumulations. CD experiments were performed by adding portions of compound stock solution into the solution of polynucleotide (c = 1-2×10^{-5} M).

Thermal melting experiments were performed on a Varian Cary 100 Bio spectrometer in quartz cuvettes (1 cm). The measurements were done in aqueous buffer solution at pH 5 or pH 7 (sodium citrate/HCl buffer I = 0.03 M). Thermal melting curves for ds-DNA, ds-RNA and their complexes with 1-4 were determined by following the absorption change at 260 nm a function of temperature.[55,56] Absorbance scale was normalized. Tm values are the midpoints of the transition curves determined from the maximum of the first derivative and checked graphically by the tangent method. The ΔTm values were calculated subtracting Tm of the free nucleic acid from Tm of the complex. Every ΔTm value here reported was the average of at least two measurements. The error in ΔTm is ± 0.5 °C.

Synthetic procedures

Boc-Lys(Boc)-Leu-Leu-Gly-AlaP-OMe (4)

Boc-Lys(Boc)-Leu-Leu-Gly-OH (**3**) (32 mg, 0.051 mmol) was dissolved in dry DMF, NMM (8 µL, 0.051 mmol) and HATU (22 mg, 0.056 mmol) were added and reaction was stirred at room temperature. After 15 min solution of H-AlaP-OMe (20 mg, 0.051 mmol) and NMM (8 µL, 0.051 mmol) in 2 mL dry DMF was added. Reaction was stirred at room temperature overnight. Solvent was evaporated and the residue purified by the flash column chromatography in EtOAc:petrol ether:EtOH 3:1:0.5.

Yield: 54 % (25 mg). Yellow oil. R_f 0.77 (EtOAc:petrol ether:EtOH 3:1:0.5). M_r 906.12. ESI-MS: *m/z* 906.5 $[M+H]^+$. ^{1}H NMR (600 MHz, CD_3OD): δ 7.63–7.56 (m, 7H H_{ar} AlaP), 4.89 (m, 1H, α AlaP), 4.10 (m, 1H, α Lys), 3.96–3.82 (m, 2H, α Leu^2, Leu^3,), 3.74 (s, 2H, α Gly), 3.35 (s, 3H, OCH_3), 3.06 (m, 2H, β AlaP), 3.03 (m, 2H, ε Lys), 1.73–1.55 (m, 10H, β,δ Lys, β,γ Leu^2, Leu^3), 1.45–1.42 (m, 18H, CH_3 Boc), 1.33 (m, 2H, γ Lys), 0.99–0.94 (m, 6H, δ,δ' Leu^2), 0.90–0.84 (m, 6H, δ,δ' Leu^3).

H-Lys-Leu-Leu-Gly-AlaP-OH (1)

Compound **4** (46 mg 0.051 mmol) was dissolved in 5 mL of methanol and 1M NaOH (105 µL, 0.105 mmol) was added. Reaction was stirred under reflux for 2 h. Solvent was evaporated, residue dissolved in water, acidified to pH 3 by 10 % citric acid and product extracted with EtOAc. After solvent evaporation, residue was dissolved in 0.5 mL of TFA-H_2O mixture (9:1, v/v) and the reaction was stirred at room temperature for 1h. Solvent was evaporated and product purified by RP-HPLC. HPLC conditions: Eurospher 100 RP C-18 column 250 × 4.5 mm, i.d. 5 µm; flow rate = 1 mL/min; λ = 270 nm; mobile phase: 0 min 40 % B, 0-20 min 40 % B-90 % A, 20-30 min 90 % B, 30-35 min 90 % B-40 % B. A = 0.1 % TFA in water, B = 0.1 % TFA in MeOH.

Yield: 67 % (12 mg). Colorless oil. R_t 19.0 min. M_r 691.86. ESI-MS: *m/z* 346.8 $[M+H]^{2+}$, *m/z* 692.4 $[M+H]^+$. ^{1}H NMR (600 MHz, CD_3OD): δ 8.94 (d, *J* = 8.6 Hz, 1H), 8.49 (d, *J* = 7.5 Hz, 1H), 8.51 (m, 1H), 8.21 – 8.16 (m, 2H), 8.00 (d, *J* = 7.0 Hz, 1H), 7.96 (d, *J* = 6.3 Hz, 1H), 4.93 (m, 1H), 4.47 (m, 1H), 4.33–4.24 (m, 1H), 3.95 (m, 1H), 3.90–3.78 (dd, ^2J = 16.9 Hz 2H), 3.38 (s, 3H), 3.36 (s, 2H), 2.99 (m, 2H), 1.91 (m, 2H), 1.78–1.69 (m, 4H), 1.64 (m, 3H), 1.58–1.48 (m, 3H), 1.00–0.86 (m, 12H). ^{13}C NMR (151 MHz, CD_3OD): δ 174.9, 174.7, 174.2, 171.2, 170.0, 162.8, 141.1, 138.8, 138.5, 134.3, 133.7, 133.2, 132.2, 130.4, 125.8, 125.5, 125.9, 124.6, 54.7, 53.9, 53.7, 53.4, 43.2, 41.7, 41.4, 40.2, 38.6, 32.0, 28.0, 25.8, 25.7, 23.4, 23.2, 22.4, 22.0, 21.8, 20.2. HRMS (MALDI-TOF/TOF): calcd. for $C_{37}H_{53}N_7O_6$ $[M+H]^+$ 692.4130; found 692.415.

Boc-Lys(Boc)-hLeu-Leu-Gly-AlaP-OMe (6)

Compound **5** (85 mg, 0.14 mmol) was dissolved in dry DMF, NMM (15 µL, 0.14 mmol) and HATU (58 mg, 0.15 mmol) were added. After 15 min solution of H-Gly-AlaP-OMe (65 mg, 0.14 mmol) and NMM (15 µL, 0.14 mmol) in 1 mL dry DMF was added. Reaction was stirred at room temperature overnight. Solvent was evaporated and the residue purified by flash column chromatography in EtOAc:petrol ether:EtOH 3:1:0.5.

Yield: 22 % (28 mg). Yellow oil. R_f 0.7 (EtOAc:petrol ether:EtOH 3:1:0.5). M_r 921.13. ESI-MS: *m/z* 921.8 $[M+H]^+$. ^{1}H NMR (600 MHz, CD_3OD): δ 8.69 (m, 2H), 8.38 (m, 2H), 8.08 (d, *J* = 8.3 Hz, 1H), 7.48 (dd, ^2J = 8.4 Hz, 2H), 4.94 (m, 1H), 3.92 (m, 1H), 3.89–3.81 (m, 1H), 3.78–3.74 (m, 2H), 3.57–3.50 (m, 1H), 3.45–3.32 (m, 2H), 2.99 (s, 3H), 2.86 (s, 3H), 2.85–2.82 (m, 2H), 1.84 (m, 2H), 1.74–1.67 (m, 3H), 1.62–1.55 (m, 3H), 1.53–1.47 (m, 2H), 1.47–1.38 (m, 18H), 1.18–1.09 (m, 2H), 1.00–0.80 (m, 12H).

H-Lys-hLeu-Leu-Gly-AlaP-OH (2)

Compound **6** (60 mg 0.07 mmol) was dissolved in 5 mL of methanol and 1M NaOH (130 µL; 0.13 mmol) was added. Reaction was stirred under reflux 2 h. Solvent was evaporated, residue dissolved in water, acidified to pH 3 by 10% citric acid and product extracted with EtOAc. After solvent evaporation, residue was dissolved in 0.5 mL of TFA-H_2O mixture (9:1, v/v) and the reaction was stirred at room temperature for 1h. Solvent was evaporated and product purified by RP-HPLC. HPLC-conditions: Eurospher 100 RP C-18 column 250 × 4.5 mm, i.d. 5 µm; flow rate = 1 mL/min; λ = 270 nm; mobile phase: 0 min 50 % B, 0-20 min 50 % B-90 % **A**, 20-30 min 90 % B, 30-35 min 90 % B-50 % B. A = 0.1 % TFA in water, B = 0.1 % TFA in MeOH.

Yield: 10 % (5 mg). Colorless oil. R_t 16.7 min. M_r 706.87. ESI-MS: *m/z* 707.3 $[M+H]^+$. ^{1}H NMR (600 MHz, CD_3CN): δ 8.83–8.78 (m, 2H), 8.42 (m, 1H), 8.38 (m, 1H), 8.15 (d, *J* = 8.3 Hz, 1H), 7.97–7.93 (m, 2H), 7.66 (m, 2H), 7.60 (d, *J* = 8.8 Hz, 1H), 7.50 (m, 2H), 4.80 (m, 1H), 4.34 (m, 2H), 3.88 (s, 2H), 3.56–3.54 (m, 1H), 3.32 (m, 2H), 2.95 (s, 3H), 1.68 (m, 2H), 1.65 (m, 2H), 1.57 (m, 2H), 1.53 (m, 2H), 1.46 (m, 2H), 1.34–1.32 (m, 2H), 0.97–0.93 (m, 12H). ^{13}C NMR (151 MHz, CD_3CN): δ 176.3, 175.3, 171.2, 169.2, 169.2, 161.1, 160.9, 140.6, 138.7, 137.5, 137.2, 133.9, 132.1, 131.3, 130.5, 125.4, 125.2, 124.4, 64.4, 54.6,

52.9, 51.9, 41.2, 40.4, 40.2, 37.7, 37.5, 30.9, 26.7, 25.8, 25.7, 23.2, 23.1, 22.4, 21.9, 21.5, 21.4. HRMS (MALDI-TOF/TOF): calcd. for $C_{37}H_{54}N_8O_6$ $[M+H]^+$ 707.4239; found 707.4252.

Boc-Lys(Boc)-hLeu-hLeu-Gly-AlaP-OMe (8)

Compound **7** (80 mg, 0.13 mmol) was dissolved in dry DMF, NMM (15 µL 0.13 mmol) and HATU (54 mg, 0.13 mmol) were added. After 15 min solution of H-Gly-AlaP-OMe (60 mg, 0.13 mmol) and NMM (15 µL, 0.13 mmol) in 1 mL dry DMF was added. Reaction was stirred at room temperature overnight. Solvent was evaporated and the residue purified by flash column chromatography in EtOAc:petrol ether:EtOH 3:1:0.5.

Yield: 11 % (14 mg). Yellow oil. R_f = 0.82 (EtOAc:petrol ether:EtOH 3:1:0.5). M_r 936.15. ESI-MS: *m/z* 937.9 $[M+H]^+$. ^{1}H NMR (300 MHz, CD_3OD): δ 8.74 (m, 1H), 8.27–8.00 (m, 1H), 7.93–7.30 (m, 5H), 4.97 (m, 1H), 4.25 (m, 1H), 4.19–3.90 (m, 1H), 3.88–3.75 (m, 1H), 3.74–3.41 (m, 2H), 3.40 (s, 3H), 3.20–2.88 (m, 4H), 2.87 (s, 3H), 2.07–1.54 (m, 8H), 1.48 (m, 18H), 1.45–1.29 (m, 4H), 1.10–0.86 (m, 12H, δ,δ' hLeu).

H-Lys-hLeu-hLeu-Gly-AlaP-OH (3)

Compound **8** (50 mg, 0.05 mmol) was dissolved in 5 mL methanol and 1M NaOH (110 µL, 0.11 mmol) was added. Reaction was stirred under reflux for 2 h. Solvent was evaporated, residue dissolved in water, acidified to pH 3 by 10 % citric acid and product extracted with EtOAc. After solvent evaporation, residue was dissolved in 0.5 mL of TFA-H_2O mixture (9:1, v/v) and the reaction was stirred at room temperature for 1h. Solvent was evaporated and product purified by RP-HPLC. HPLC conditions: Eurospher 100 RP C-18 column 250 × 4.5 mm, i.d. 5 µm; flow rate = 1 mL/min; λ = 270 nm; mobile phase: 0 min 50 % B, 0-20 min 50 % B-90 % **A**, 20-30 min 90 % B, 30-35 min 90 % B-50 % B. A = 0.1 % TFA in water, B = 0.1 % TFA in MeOH.

Yield: 13 % (5 mg). Colorless oil. R_t 18.1 min. M_r 721.89. ESI-MS: *m/z* 722.5 $[M+H]^{+\cdot}$ ^{1}H NMR (600 MHz, CD_3CN): δ 8.74 (m, 2H, 8.31 (d, *J* = 5.3 Hz, 1H), 8.02 (d, *J* = 8.5 Hz, 1H), 7.20 (m, 3H), 6.65 (s, 1H), 4.82 (m, 1H), 3.77–3.70 (m, 1H), 3.68 (m, 2H), 3.54–3.49 (m, 2H), 3.32 (m, 2H), 3.26 (s, 3H), 2.54 (m, 2H), 2.04 (m, 2H), 1.87–1.80 (m, 2H), 1.63 (m, 2H), 1.56–1.50 (m, 2H), 1.38–1.32 (m, 4H), 0.89–0.86 (m, 12H). ^{13}C NMR (151 MHz, CD_3CN): δ 178.1, 172.1, 171.4, 170.9, 170.1, 162.8, 141.1, 138.8, 138.5, 134.3, 134.1, 133,7, 133.2, 132.8, 131.9, 130.4, 125.8, 125.7, 124.0, 124.6, 66.3, 63.9, 57.8, 53.6, 43.5, 41.3, 40.1, 38.6, 33.8, 29.6, 25.6, 24.8, 22.8, 22.1, 22.0, 21.9, 20.2. HRMS (MALDI-TOF/TOF): calcd. for $C_{37}H_{55}N_9O_6$ $[M+H]^+$ 722.4348; found 722.4349.

Boc-Lys(Boc)-hLeu-Leu-hLeu-Gly-AlaP-OMe (10)

Boc-Lys(Boc)-hLeu-Leu-hLeu-OH (45 mg, 0.063 mmol) was dissolved in dry DMF, NMM (7 µL, 0.063 mmol) and HATU (26 mg, 0.069 mmol) were added. After 15 min solution H-Gly-AlaP-OMe (30 mg, 0.063 mmol) and NMM (7 µL, 0.063 mmol) in 1 mL dry DMF was added. Reaction was stirred at room temperature overnight. Solvent was evaporated and the residue purified by flash column chromatography in eluents EtOAc:petroleum ether:EtOH=3:1:0.5.

Yield: 61 % (40 mg). Yellow oil. R_f = 0.78 (EtOAc:petroleum ether:EtOH=3:1:0.5). M_r 1049.31. ESI-MS: *m/z* 1050 $[M+H]^+$.

H-Lys-hLeu-Leu-hLeu-Gly-AlaP-OH (4)

Compound **9** (40 mg, 0.038 mmol) was dissolved in 5 mL methanol and 1M NaOH (286 µL, 0.286 mmol) was added. Reaction was stirred under reflux for 12 h. Solvent was evaporated, residue dissolved in water, acidified to pH 3 by 10 % citric acid and product extracted with EtOAc. After solvent evaporation, residue was dissolved in 0.5 mL of TFA-H_2O mixture (9:1, v/v) and the reaction was stirred at room temperature for 1h. Solvent was evaporated and product purified by RP-HPLC. HPLC conditions: Eurospher 100 RP C-18 column 250 × 4.5 mm, i.d. 5 µm; flow rate = 1 mL/min; λ = 270 nm; mobile phase: 0 min 50 % B, 0-20 min 50 % B-90 % **A**, 20-30 min 90 % B, 30-35 min 90 % B-50 % B. A = 0.1 % TFA in water, B = 0.1 % TFA in MeOH

Yield: 10 % (3 mg). Colourless oil. R_t 23.8 min. M_r 835.05. ESI-MS: *m/z* 835.6 $[M+H]^+$. ^{1}H NMR (600 MHz, CD_3OD): δ 8.97 (m, 1H), 8.79 (m, 1H), 8.51 (dd, *J* = 8.4 Hz, 1H), 8.27–7.99 (m, 3H), 7.56 (d, ^2J = 8.4 Hz, 1H), 4.91 (m, 1H), 4.49–4.42 (m, 1H), 4.14–4.06 (m, 1H), 3.64 (m, 2H), 3.39 (s, 5H), 3.01 (m, 2H), 2.99–2.91 (m, 2H), 2.01 (m, 2H), 1.93–1.88 (m, 2H), 1.78–1.75 (m, 3H), 1.68–1.59 (m, 12H), 1.53–1.50 (m, 2H), 0.98–0.93 (m, 18H). ^{13}C NMR (151 MHz, CD_3CN): δ 178.2, 172.3, 171.6, 170.7, 170.3, 170.1, 162.8, 141.2, 138.7, 138.6, 134.3, 133.9, 132.5, 131.8, 130.4, 125.8, 125.5, 125.1, 124.7, 124.6, 66.3, 63.7, 57.6, 57.3, 55.4, 53.5, 43.7, 41.2, 40.1, 39.8 38.6, 33.5, 32.8, 29.6, 25.8, 25.5, 24.8, 24.6, 22.7, 22.4, 22.2, 21.7, 20.3. HRMS (MALDI-TOF/TOF): calcd. for $C_{43}H_{66}N_{10}O_7$ $[M+H]^+$ 835.5188; found 835.5199.

Cytotoxicity evaluation

Cytotoxic effects on the normal and tumors cells' growth were determined using the colorimetric methyltetrazolium (MTT) assay. Experiments were carried out on three tumor human cell lines (HeLa, CaCo-2, and K562) and on one canine cell line (MDCK I) as normal cells. The adherent cells, MDCK1, HeLa, and $CaCO_2$, were seeded in 96 micro-well plates at a concentration of 2×10^4 cells/mL and allowed to attach overnight in the CO_2 incubator (IGO 150 CELLlife^{TM}, JOUAN, Thermo Fisher Scientific**,** Waltham, MA, USA). After 72 hours of exposure to tested compounds, medium was replaced with 5 mg/mL MTT solution and the resulting formazane crystals were dissolved in DMSO. Leukemia cells at a concentration of $1x10^5$ cells / mL, were plated onto 96 micro-well plates and after 72 hours of incubation, 5mg/mL MTT solution was added to each well and incubated 4 hours in CO_2 incubator. To each well, 10% SDS with 0.01 mol / L HCl was added to dissolve water-insoluble MTT-formazane crystals overnight. Elisa micro plate reader (iMark, BIO RAD, Hercules, CA, USA) was used for measurement of absorbance at 595nm. All experiments were performed at least three times in triplicates. The percentage of cell growth (PG) was calculated using the following equation:

$PG= (A_{compound} - A_{background} / A_{control} - A_{background}) X100$

where $A_{background}$ at the adherent cells is absorbance of MTT solution and DMSO; $A_{background}$ at the suspension cells is the absorbance of the medium without cells, but containing MTT

and 10%SDS with 0.01 mol/L HCl; and $A_{control}$ is the absorbance of cell suspension grown without tested compounds.

Acknowledgements

This work has been supported by Croatian Science Foundation projects 1477 and 3102. The support from FP7-REGPOT-2012-2013-1 project, Grant Agreement Number 316289 – InnoMol is gratefully acknowledged.

Notes and references

1 Y. Zhao, A. Aguilar, D. Bernard, S. Wang, *J. Med. Chem.,* 2015, **58**, 1038.
2 A. Domling, *Curr. Opinion Chem. Biol*., 2008, **12**, 281.
3 J. D. A. Tyndall, B. Pfeiffer, G. Abbenante, D. P. Fairlie, *Chem. Rev.* 2005, **105**, 793.
4 T. A. Hill, N. E. Shepherd, F. Diness, D. P. Fairlie, *Angew. Chem. Int. Ed.,* 2014, **53**, 2.
5 J. M. Smith, J. R. Frost, R. Fasan, *Chem. Commun.***,** 2014, **50**, 5027.
6 J. K. Murray, S. H. Gellman, *Peptide Sci*., 2007, **88**, 657.
7 L. Nevola, E. Giralt, *Chem. Commun.***,** 2015, **51**, 3302.
8 I. Avan, C. D. Hallb, A. R. Katritzky, *Chem. Soc. Rev.,* 2014, **43**, 3575.
9 P. G. Vasudev, S. Chatterjee, N. Shamala, P. Balaram. *Chem. Rev.* 2011, **111**, 657.
10 D. Seebach, J. Gardiner, *Acc. Chem. Res.,* 2008, **41**, 1366.
11 A. D. Bautista, J. S. Appelbaum, C. J. Craig, J. Michel, A. Schepartz, *J. Am. Chem. Soc.,* 2010, **132**, 2904.
12 E. V. Denton, C. J. Craig, R. L. Pongratz, J. S. Appelbaum, A. E. Doerner, A. Narayanan, G. I. Shulman, G. W. Cline and A. Schepartz, *Org. Lett.,* 2013, **15**, 5318.
13 A. Cheguillaume, A. Salaün, S. Sinbandhit, M. Potel, P. Gall, M. Baudy-Floch, P. Le Grel, J. *Org. Chem.,* 2001, **66**, 4923.
14 S. Acherar, A. Salaün, P. Le Grel, B. Le Grel, B. Jamart-Grégoire, *Eur. J. Org. Chem.,* 2013, 5603.
15 (a) M. Laurencin, M. Amor, Y. Fleury, M. Baudy-Floc'h, *J. Med. Chem.,* 2012, **55**, 10885; (b) M. Laurencin, B. Legrand, E. Duval, J. Henry, M. Baudy-Floc'h, C. Zatylny-Gaudin, A. Bondon, *J. Med. Chem.,* 2012, **55**, 2025.
16 A. Bordessa, M. Keita, X. Maréchal, L. Formicola, N. Lagarde, J. Rodrigoa, G. Bernadat, C. Bauvais, J.L. Soulier, L. Dufau, T. Milcent, B. Crousse, M. Reboud-Ravauxb, S. Ongeri, *Eur. J. Med. Chem.,* 2013, **70**, 505.
17 (a) J. Suć, I. Jerić, *SpringerPlus* 2015, **4**, 507; (b) S. S. Panda, C. El-Nachef, K. Bajaj, A. R. Katritzky, *Eur. J. Org. Chem.,* 2013, **19**, 4156.
18 J. Matić, L.-M. Tumir, M. Radić Stojković, i Piantanida, *Curr. Prot. Pep. Sci.,* 2016, **17**, 127.
19 a)A. L. Stewart and M. L. Waters, *Chembiochem* 2009, **10**, 539-544.; b) L. L. Cline and M. L. Waters, *Org. Biomol. Chem.* 2009, **7**, 4622-4630
20 L.-M. Tumir, I. Piantanida, P. Novak, M. Žinić, *J. Phys. Org. Chem.,* 2002, **15**, 599.
21 L.-M. Tumir, I. Piantanida, I. Juranović, Z. Meić, S. Tomić, M. Žinić, *Chem. Commun.* 2005, 2561.
22 a) M. Dukši, D. Baretić, V. Čaplar, I. Piantanida, *Eur. J. Med. Chem.,* 2010, **45**, 2671; b) M. Dukši, D. Baretić, I. Piantanida, *Acta Chim. Slov.,* 2012, **59**, 464.
23 A. Rodger, B. Norden, *Circular Dichroism and Linear Dichroism*; Oxford University Press: New York, **1997**, Chap. 2.
24 N. Berova, K. Nakanishi, R. W. Woody, *Circular Dichroism Principles and Applications*, 2nd edn, New York Wiley-VCH, 2000.
25 M. Eriksson, B. Nordén, *Methods Enzymol.,* 2001, **340**, 68.
26 a) G. Scatchard, The attractions of proteins for small molecules and ions, *Ann. N.Y. Acad. Sci.,* 1949, **51**, 660; b) J.D. Mc Ghee, P.H. von Hippel, Theoretical aspects of DNA-protein interactions: Co-operative and non-co-operative binding of large ligands to a one-dimensional homogeneous lattice, *J. Mol. Biol.,* 1974, **86** 469.
27 M. Demeunynck, C. Bailly and W. D. Wilson, Small Molecule DNA and RNA Binders: From Synthesis to Nucleic Acid Complexes, Wiley-VCH Verlag GmbH & Co. KGaA, 2004.
28 E. Garcia-Espana, I. Piantanida, H. J. Schneider, Nucleic Acids as Supramolecular Targets, Royal Society of Chemistry, London, 2013.
29 A. Cheguillaume, A. Salau, S. Sinbandhit, M. Potel, P. Gall, *J. Org. Chem.,* 2001, **66**, 4923.
30 A. Salaün, A. Favre, B. Le Grel, M. Potel, P. Le Grel, *J. Org. Chem,.* 2006, **71**, 150.
31 G. Lelais, D. Seebach, *Helv. Chim. Acta* 2003, **86**, 4152
32 K. Gröger, D. Baretić, I. Piantanida, M. Marjanović, M. Kralj, M. Grabar, S. Tomić, C. Schmuck, *Org. Biomol. Chem.,* 2011, **9**, 198.
33 W. Humphrey, A. Dalke, K. Schulten, VMD - Visual Molecular Dynamics" *J. Molec. Graphics* 1996, **14**, 33.
34 C. R.Cantor, P. R. Scimmel, *Biophysical Chemistry*, vol. 3,. WH Freeman and Co., San Francisco, 1980, pp 1109-1181.
35 R. Günther, H. J. Hofmann, *J. Am. Chem. Soc.* 2001, **123**, 247.
36 W. S. Horne, S. H .Gellman, *Acc. Chem. Res.* 2008, **41**, 1399.
37 T. A. Martinek, F. Fülöp, *Chem. Soc. Rev*. 2012, **41**, 687.
38 S. H. Choi, I. A. Guzei, L. C. Spencer, S. H. Gellman, *J. Am. Chem. Soc.,* 2009, **131**, 2917.
39 W. S. Horne, L. M. Johnson, T. J. Ketas, P. J. Klasse, M. Lu, J. P. Moore, S. H. Gellman, *Proc. Nat. Acad. Sci. USA,* 2009, **106**, 14751.
40 Z. Hegedüs, E. Wéber, E. Kriston-Pál, I. Makra, A. Czibula, E. Monostori, T. A. Martinek, *J. Am. Chem. Soc.* 2013, **135**, 16578.
41 B. J. Smith, E. F. Lee, J. W. Checco, M. Evangelista, S. H. Gellman, W. D. Fairlie, *Chembiochem* 2013, **14**, 1564.

42 H. S. Haase, K. J. Peterson-Kaufman, S. K. Lan Levengood, J. W. Checco, W. L. Murphy, S. H. Gellman, *J. Am. Chem. Soc.* 2012, **134**, 7652.
43 L. Nevola, E. Giralt, *Chem. Commun*. 2015 **51**, 3302.
44 L.-M. Tumir, M. Radić Stojković, I. Piantanida, *Beilstein J. Org. Chem.,* 2014, **10**, 2930.
45 L.-M. Tumir, M. Radić-Stojković and I. Piantanida, *Beilstein J. Org. Chem.,* 2014, **10**, 2930–2954
46 a) J. Lhomme, J. F. Constant and M. Demeunynck, *Biopolymers,* 1999, **52**, 65-83; b) A. Martelli, J. F. Constant, M. Demeunynck, J. Lhomme and P. Dumy, *Tetrahedron,* 2002, **58**, 4291.
47 B. M. Zeglis, J. A. Boland and J. K. Barton, *Biochemistry* 2009, **48**, 839-849
48 S. M. Butterfield, W. J. Cooper and M. L. Waters, *J. Am. Chem. Soc.* 2005, **127**, 24-25
49 S. T. Meyer and P. J. Hergenrother, *Org. Lett*. 2009, **11**, 4052-4055
50 H. J. Xi, D. Gray, S. Kumar and D. P. Arya, *Febs Letters* 2009, **583**, 2269-2275.
51 J. B. Chaires, N. Dattagupta, D. M. Crothers, *Biochemistry,* 1982, **21**, 3933.
52 G. Malojčić, I. Piantanida, M. Marinić, M. Žinić, M. Marjanović, M. Kralj, K. Pavelić, H.-J. Schneider, *Org. Biomol. Chem.* 2005, **3**, 4373.
53 C. Ciatto, M. L. D'Amico, G. Natile, F. Secco, M. Venturini *Biophys. J.* 1999, **77**, 2717.
54 A. Das, K. Bhadra, B. Achari, P. Chakraborty, G. S. Kumar, *Biophys. Chem.,* 2011, **155**, 10.
55 I. Piantanida, B. S. Palm, M. Žinić, H.-J. Schneider, *J. Chem. Soc., Perkin Trans. 2*, 2001, 1808.
56 J. L. Mergny, L. Lacroix, *Oligonucleotides*, 2003, **13**, 515.